

Effect of Wheels, Casters and Forks on Vibration Attenuation and Propulsion Cost of Manual Wheelchairs

Jacob P. Misch¹, Member, IEEE, Yuanning Liu, and Stephen Sprigle

Abstract—Manual wheelchair users are exposed to whole-body vibrations as a direct result of using their wheelchair. Wheels, tires, and caster forks have been developed to reduce or attenuate the vibration that transmits through the frame and reaches the user. Five of these components with energy-absorbing characteristics were compared to standard pneumatic drive wheels and casters. This study used a robotic wheelchair propulsion system to repeatedly drive an ultra-lightweight wheelchair over four common indoor and outdoor surfaces: linoleum tile, decorative brick, poured concrete sidewalk, and expanded aluminum grates. Data from the propulsion system and a seat-mounted accelerometer were used to evaluate the energetic efficiency and vibration exposure of each configuration. Equivalence test results identified meaningful differences in both propulsion cost and seat vibration. LoopWheels and SoftWheels both increased propulsion costs by 12-16% over the default configuration without reducing vibration at the seat. Frog Legs suspension caster forks increased vibration exposure by 16-97% across all four surfaces. Softroll casters reduced vibration by 11% over metal grates. Wide pneumatic ‘mountain’ tires showed no difference from the default configuration. All vibration measurements were within acceptable ranges compared to health guidance standards. Out of the component options, softroll casters show the most promising results for ease of efficiency and effectiveness at reducing vibrations through the wheelchair frame and seat cushion. These results suggest some components with built-in suspension systems are ineffective at reducing vibration exposure beyond standard components, and often introduce mechanical inefficiencies that the user would have to overcome with every propulsion stroke.

Index Terms—Manual wheelchairs, vibrations, propulsion cost, energy loss, standards.

Manuscript received 3 March 2022; revised 10 May 2022 and 15 August 2022; accepted 6 September 2022. Date of publication 9 September 2022; date of current version 22 September 2022. This work was supported in part by the National Institute on Disability, Independent Living, and Rehabilitation Research under Grant 901FRE0036, in part by the Rehabilitation Engineering and Applied Research Laboratory through internal funding, and in part by the School of Industrial Design at Georgia Institute of Technology through internal funding. (Corresponding author: Jacob P. Misch.)

Jacob P. Misch and Yuanning Liu are with the Rehabilitation Engineering and Applied Research Laboratory, School of Mechanical Engineering, Georgia Institute of Technology, Atlanta, GA 30332 USA (e-mail: mischjp@gatech.edu; yliu3217@gatech.edu).

Stephen Sprigle is with the Rehabilitation Engineering and Applied Research Laboratory, the School of Mechanical Engineering, and the School of Industrial Design, Georgia Institute of Technology, Atlanta, GA 30332 USA (e-mail: stephen.sprigle@design.gatech.edu).

Digital Object Identifier 10.1109/TNSRE.2022.3205507

I. INTRODUCTION

HUMANS are often exposed to vibrations through extraneous sources during activities of daily life within and outside the household, and especially in the workplace. In certain doses, vibration exposure has been correlated to positive effects on physiological health [1], [2]. In other situations, deleterious health effects are instead attributed to the vibration, namely in the form of neck and lower back pain [3], [4] and fatigue [5] in seated persons in the workplace. To combat the health risks from workplace vibration exposure, organizations including the International Standards Organization (ISO) and the Health and Safety Executive (HSE) in the United Kingdom have developed guidelines and thresholds for potential health risks associated with an 8-hour duration of whole-body vibration (WBV) exposure [6], [7]. Magnitudes and frequencies of the vibrations, as well as the durations of exposure, are considered in these assessments. However, as these guidelines were developed around the comfort of only seated, able-bodied humans in the workplace, they may not appropriately reflect permissible vibration exposure levels for non-able-bodied individuals performing everyday activities.

Manual wheelchair (MWC) users are exposed to WBV directly from the use of their wheelchair. While there are no conclusions about the full extent of adverse health effects from MWC-induced WBV [8], some common ailments and comorbidities of MWC users such as lower back pain [3], neck pain [9] and fatigue [10] may be explained by constant WBV exposure, and many wheelchair users have spinal impairments that could explain symptom onset for a low amount of vibration exposure. Several articles contend that WBV exposure levels of MWC users are non-negligible [8], [10], [11], [12], [13], [14]. However, research suggests that the duration of time moving in a manual wheelchair is very low, on the order of 1 hour per day [15], [16], [17], compared to the 8-hour exposure period used by ISO and HSE. Since vibration exposure is based upon time of exposure, the implication for users remains unclear.

Few studies to date [12], [13], [14], [18] have reported harmful MWC vibration exposure levels. Garcia-Mendez *et al.* [14] calculated WBV from total daily occupancy time (13 hours). This implies 12 hours of vibration exposure, on average, occurred when the user was occupying but not propelling the wheelchair. While MWC users may also experience vibrations when they are not in

motion (e.g., riding in a car or bus), these vibrations should not be conflated with those incurred through direct wheelchair usage (i.e., self-propulsion) alone, and could be reported separately. Other studies [12], [13], [18] report WBV values that require ≥ 2.3 hours of daily travel (i.e. considerably higher than the daily average) over tactile surfaces (e.g. exterior concrete or brick walkways) to reach harmful WBV levels. Regardless of health effects, vibration measurements may help inform design of wheelchair components to promote comfort and ease of use in various environments.

Commercially-available products have been evaluated for their efficacy in reducing shock and vibration transmission through the MWC frame. Caster forks with built-in vertical suspensions are reported to decrease peak accelerations at both the seat and footrest [11] using double-drum tests. One suspension frame (Quickie XTR) also demonstrated superior vibratory power dissipation to cross-brace folding frames for curb descents [19]. Utilizing human occupants as subjects introduces biomechanical complexity, as the resonant frequencies of human bodies (between 4-12 Hz) [20] differ from those of wheelchair frames (20-30 Hz) [21], and the occupant may anticipate and pre-emptively adapt postures to minimize vibrations and shocks [22]. However, the use of human occupants in over-ground tests have obvious relevance to real-world use and the utility of these MWC components.

Wheelchair performance needs to be evaluated by measuring the effect of suspension systems not just on vibration attenuation, but also on the efficiency of propulsion. MWC self-propulsion is inherently inefficient and repetitive overexertion can cause injuries within the upper extremities from excessive joint torques and forces [23], [24], [25]. Reduced mobility can hinder community participation [17], which can lead to physiological and mental detriments from inactivity and isolation [26], [27], [28], and sedentary periods in a seated posture is correlated with risks of pressure injuries [29]. Recent research has delved into component-based performance metrics to quantify the general energy loss parameters (rolling resistance, scrub torque) [30] and the corresponding impact on the system-level wheelchair propulsion cost [31]. Theoretically, the same energy absorption abilities that are beneficial for vibration attenuation may also absorb some of the energy exerted to impart motion, effectively reducing the mechanical efficiency of the wheelchair and increasing the cost of propulsion. The ideal configuration should absorb vibratory energy when traveling over rough surfaces without incurring added propulsion cost when traveling over smooth ground.

To date, only two studies have proposed frameworks to compare MWC vibration parameters with energetic analogues to propulsion costs using human subjects [12], [32]. Cooper *et al.* [12] measured vibrations in manual and power wheelchairs over selected sidewalk surfaces and average work for propulsion of the MWCs. Differences were found between vibration exposures of the wheelchair types and the sidewalk surfaces, but no differences were found between energy requirements between surfaces, attributed to the similar surface characteristics and flatness of the test track. Chénier and Aissaoui set out to compare MWC frame materials (aluminum, titanium, carbon fiber) with respect to vibration transmissibility and mechanical work per meter traveled. Human subjects

propelled across three test tracks with standardized wheels and tires. Their findings support the vibration attenuation capabilities of carbon fiber and, though no significant difference in propulsion cost were reported, negative correlations present in the data analysis suggest that frame-based energy absorption reduces vibration exposure at the likely expense of mechanical propulsion efficiency [32]. Optimization of MWCs require careful assessment of the anticipated environments of use, as propulsion cost and vibration exposure can vary across surfaces, as well as between configurations of tires and weight distributions.

The objective of this study is to assess the impact of five commercially-available components on propulsion cost and vibration exposure, as measured at three locations on the wheelchair frame. The breadth of measurement is vital to identify the potential benefit of vibration attenuation in relation to the potential for added propulsion cost. Four common indoor and outdoor surfaces were selected that represent a wide range of commonly-traveled surfaces: decorative brick, expanded aluminum grates, sidewalk, and linoleum tile. These surfaces were chosen because they induce steady-state vibrations (i.e., experienced *every single time* the wheelchair is in motion), rather than the comparatively infrequent low-frequency, high-magnitude shocks or impacts experienced by users (e.g., traversing thresholds, curb-drops, and potholes). A wheelchair-propelling robotic testbed was used to drive each configuration with highly repeatable trajectories to standardize the travel path, maneuver speed, and weight distribution over the components to permit accurate measurements of the propulsion costs as reported in prior work [33].

II. HARDWARE AND CONFIGURATIONS

Experimental methods involved assessing the propulsion cost and vibration exposure of one MWC in six configurations.

A. Wheelchair Testing

The Anatomical Model Propulsion System (AMPS), shown in Figure 1, is a wheelchair-propelling robot that was used to maneuver the wheelchair in this study. Its propulsion subsystem permits highly repeatable, configurable propulsion patterns to be deployed across a wide range of chair configurations. Its construction mimics a seated person in size, shape, and mass distribution to apply realistic loads to the frame and wheels as per the wheelchair test dummy standard defined by ISO 7176-11 [34], scaled to a total mass of 80 kg to more closely represent the average occupant mass reported in [35]. Wheelchair propulsion is controlled by motors attached to custom-made ring gears replacing the push-rims of each drive wheel. A high-powered motor speed controller (HDC 2460, RoboteQ Inc.) utilizes velocity-based feedback system to impart discrete and highly repeatable pushes. Between pushes, the motors are mechanically disconnected from the push-rims, allowing the wheelchair to freely coast. Rotational speed of each drive wheel is collected from axle-mounted optical encoders (EM1-2500-I, US Digital Inc.) fixed to the drive wheel axles. Wheel torques are derived from the armature current of each motor, measured with Hall-effect current sensors (DFRobot SEN0098, Zhiwei Robotics Corp.). Signals



Fig. 1. The wheelchair-propelling robot used to control maneuvers in this study.

Component Name	Wheel View (Top View)	Tire Profile (Profile View)	Mass (kg)	Tire Hardness (Type A Durometer)
24x1-3/8" Primo Orion Pneumatic (75 psi) Metal spoked wheel			1.86	67
24x2.10" Mountain Wheel Pneumatic (55 psi) Metal spoked wheel			2.04	57
24x1-3/8" Primo Orion Pneumatic (75psi) LoopWheel			2.61	67
24x1-3/8" Primo Orion Pneumatic (75psi) SoftWheel			2.89	67
5x1" Primo Solid Caster Wheel			0.22	85
5x1.5" Primo Soft Roll Solid Caster Wheel			0.39	65

Fig. 2. Component selection showing measurements and views of each wheel and tire.

are sampled at 40 Hz by an on-board data acquisition system (USB-6341, National Instruments Corp.). More details of the design and overview can be found in the original design article by Liles *et al.* [36].

B. Components and Wheelchair Configurations

One rigid aluminum ultra-lightweight wheelchair frame (Rogue, Ki Mobility) was used for all trials, with 0° camber, 3° seat dump, and 87° back angle. The chair was configured with six unique combinations of drive wheels, caster wheels, and caster forks. Component options comprised four drive wheels and two sets of caster wheels, shown Figure 2. The ‘default’ configuration was defined to have 24 × 1.3/8” pneumatic

TABLE I
COMPONENTS AND CHARACTERISTICS FOR EACH CONFIGURATION

Name	Drive Wheel	Drive Tire	Caster Fork	Caster Wheel	Mass (kg)	WD (%)
Default	Metal Spoked (Default)	Primo Orion (Default)	Rigid Alum. (Default)	Primo 5x1" (Default)	94.5	69.1
Softroll	Default	Default	Default	Primo 5x1.5" Softroll	94.7	68.4
SoftWheel	Softwheel	Default	Default	Default	96.8	69.4
LoopWheel	Loopwheel	Default	Default	Default	96.3	70.7
MtnWheel	Default	24x2.10" Mountain wheel	Default	Default	95.2	68.9
FrogLegs Forks	Default	Default	Frog Legs Suspension Fork	Default	96.0	69.8



Fig. 3. (Left) Default rigid aluminum and (right) Frog Legs suspension caster forks.

tires (Primo Orion, Xiamen Lenco Co., Ltd.) inflated to the recommended 75 psi on metal spoked drive wheels, and solid 5 × 1” urethane caster wheels (Primo 5 × 1, Xiamen Lenco Co., Ltd.). These components served as the basis of comparison as they are common standard options offered by manufacturers at no additional cost to the user.

The chosen ‘energy-absorbing’ components were selected based on their assumed dampening capabilities, and would incur additional monetary cost to add to any user’s wheelchair configuration. These included: 24 × 2.10” mountain tires on 22” spoked wheels (Mountain Wheel Complete, Part #762017, Sunrise Medical, Inc.); the default tires on LoopWheels (LoopWheel Urban, Jelly Products Ltd.) with ‘regular’ stiffness settings; the default tires on SoftWheels (Acrobat A, SoftWheel Ltd.) with Stage 4 shocks; and compliant Soft Roll casters (Caster 5” Soft Roll, Part #400103, Sunrise Medical, Inc.). While SoftWheels are no longer commercially available in the U.S., the closest equivalent international model is the SoftWheel 3.0 with Stage C shocks.

Figure 3 shows the rigid aluminum forks equipped by default on the wheelchair frame and a pair of suspension forks with an interchangeable wedge-shaped damper element (Frog Legs II Suspension Forks, Frog Legs Inc.). The default forks were used in five of the six configurations.

When testing a drive wheel, the standard 5 × 1” caster was used, and when testing a caster component, the standard 24 × 1.3/8” pneumatic tired was used. Mass and weight

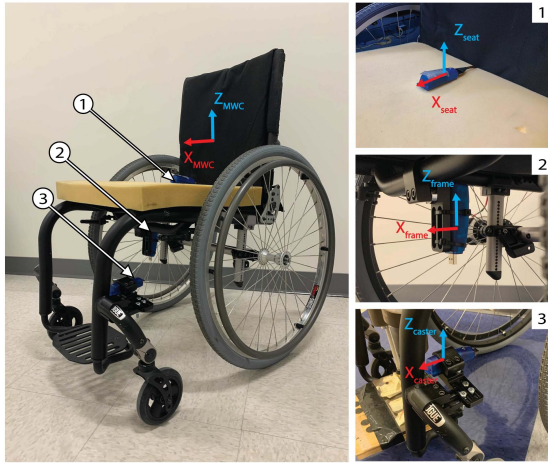


Fig. 4. Views of each triaxial accelerometer mounting location and primary axes.

distribution (WD), reported as percent total mass over the drive wheel axle, are shown for each configuration.

C. Vibration Monitoring

Triaxial accelerometers (X16-1D, Gulf Coast Data Concepts) with ± 16 g ranges and user-selectable sampling rates of 12 – 3200 Hz were used to measure vibration data on the wheelchair. Three X16-1D accelerometers were fastened to the wheelchair at: (1) the top surface of the wheelchair cushion; (2) the rigid frame member beneath the seat; (3) the frame member connecting the caster forks to the main frame (Figure 4). The primary axes of the wheelchair were globally defined with the x-axis representing antero-posterior, y-axis for medio-lateral, and z-axis for vertical directions. These are the directions that vibrations enter the seated body, as in ISO 2631-1 [6].

The accelerometers were oriented such that direct acceleration measurements at each location could be converted into accelerations along each global primary axis. Each accelerometer sampled at 200 Hz. Trial start and end points were synchronized across accelerometers. Measurements were recorded for all axes. Only the measurements in the global vertical axis was used for analysis, as it has the largest component of surface-related vibration magnitude [10], [12], [32], and is the direction most closely associated with discomfort [37] and physiological injury [5], [9].

The accelerometer near the caster captured the most severe vibrations [11], [38], as the casters are the first component to interact with surface inconsistencies and their small radius magnifies the force of impact with any obstacles compared to the larger radius of the drive wheels [39]. Caster vibrations were compared between the Default and caster configurations (Softroll, FrogLegs Forks). The frame-mounted accelerometer measured the vibrational input from the interactions between the drive wheels and the surfaces, and was used to compare the drive wheel configurations (SoftWheel, LoopWheel, MtnWheel) against the Default. The seat accelerometer measured the overall vibration that would reach the user, as a culmination of vibrations from the casters and drive wheels, as well as the transmissibility through the wheelchair

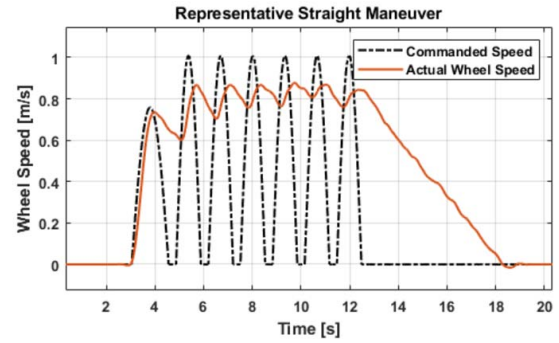


Fig. 5. Commanded wheel speeds (dotted line) and representative measured wheel speeds (solid line) for one over-ground trial.

frame [32] and the cushion [40]. Measurements at the seat were compared for all six configurations.

D. Maneuver Selection

Wheelchair use can involve an infinite number of maneuvers with various speeds and radii of curvature, though typical bouts of mobility are short (<20 s) and slow (<0.44 m/s) with frequent stops, starts, and turns [16], [17] at low speeds. Travel-induced vibrations are expected to occur at greater magnitudes at higher travel speeds with all four wheels rolling over the ground. Turning maneuvers, therefore, are expected to be less likely to induce vibrations as they occur at slow speeds over short distances. A 'Straight' maneuver was developed to drive the chair in a straight line at a realistic steady-state speed of 1.0 m/s. Wheel trajectories (Figure 5) include two initial pushes to accelerate the wheelchair, five pushes to maintain travel speed between 0.8 m/s to 1.0 m/s, and a coast down period to naturally decelerate the chair to a complete stop. Similar travel speeds were used in prior studies on propulsion cost [33], [41] as well as vibration exposures of human subjects [15], [32]. Travel started at the same position for each tested configuration. Distance for each trial was approximately 10 meters on average and varied slightly between trials and configurations.

III. METHODS

A. Data Collection

Tests were conducted on four surface types: decorative brick, expanded aluminum grates, sidewalk, and linoleum tile, collectively seen in Figure 6. To account for any slopes or inconsistencies in each surface, 6 trials were run in opposing directions along the same path for a total of 12 trials per surface per configuration, or 288 trials overall. Data from the motor armature current sensors, motor encoders, and wheel-mounted encoders were collected at 40 Hz during the over-ground trials. These data were processed in MATLAB (R2020a, The Mathworks Inc.).

B. Propulsion Cost Calculation

Propulsion cost reports the amount of energy exerted by the AMPS to perform a maneuver, normalized by the distance traveled by the wheelchair. Lower propulsion cost indicates greater efficiency. The calculation of propulsion cost is derived

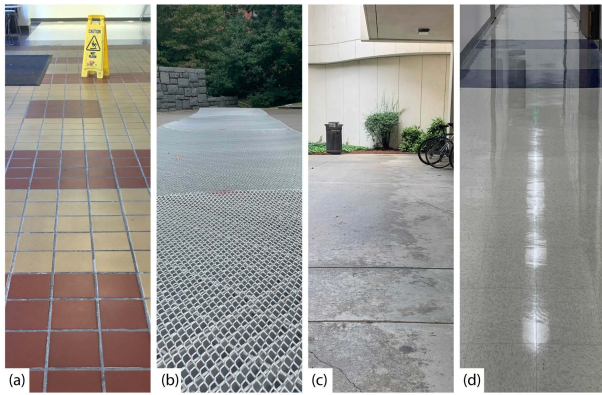


Fig. 6. Test surfaces included (a) decorative interior brick, (b) expanded aluminum grates, (c) poured concrete sidewalk, and (d) smooth interior tile.

from the fundamental theorems of work-energy. The propulsion torques on each wheel (τ_L , τ_R) are calculated from the measured motor armature current and scaled by the gear ratio between the motor pinion and the custom push-rim, as in Liles *et. al* [36]. Rotational power is then found by multiplying the wheel torque by the corresponding wheel speed (ω_L , ω_R), measured with the hub-mounted optical encoders. Total work supplied to the chair is then calculated by integrating the sum of the left and right rotational powers over the duration of the maneuver, from the start time (t_i) to the end time (t_f). Finally, the propulsion cost value is calculated by dividing the total work supplied to the chair, in Joules, by the linear displacement or distance traveled by the center of mass (Δs), in meters.

$$\text{Propulsion Cost} = \frac{\int_{t_i}^{t_f} (\tau_L \omega_L + \tau_R \omega_R) dt}{\Delta s} \quad (1)$$

C. Vibration Analysis

Vibration measurements from each accelerometer were saved into separate files for each over-ground trial. A custom MATLAB algorithm imported and normalized the data by subtracting the baseline mean values for each axis. Trials were trimmed to include only the 'steady-state' phase of the maneuver (i.e. after the first two 'acceleration' pushes until the end of the last push, excluding the final coast-down). The primary outcome variable was root-mean-squared (r.m.s.) acceleration, calculated by integrating the squared z-axis acceleration data (a_z) over the maneuver duration with the following equation:

$$a_{z,r.m.s.} = \left[\left(\frac{1}{t_f - t_i} \right) \int_{t_i}^{t_f} (a_z^2) dt \right]^{\frac{1}{2}} \quad (2)$$

D. Statistical Analysis

Descriptive statistics (mean, standard deviation) were calculated for propulsion cost and seat, frame, and caster vibrations across all configurations and surfaces. Further analysis involved comparisons of outcome variables for each tested configuration to those of the Default configuration. Equivalence testing is a technique used to assess whether responses (e.g., propulsion cost values) differ between groups by more

than a practically-important amount (e.g., $H_0 : \mu_A - \mu_B \leq \delta_1$ and $H_0 : \mu_A - \mu_B \geq \delta_2$) through the use of two one-sided t-tests against user-defined bounds (δ_1 , δ_2). This approach is often more appropriate than inferring a lack of a difference (e.g., $H_0 : \mu_A = \mu_B$ or $\Delta = 0$) when assessed by traditional statistical means [42], [43], because the upper and lower equivalence limits are based on meaningful values, often informed by related studies in the literature. While a formal equivalence test was not directly used here, the underlying premise and computational approach was adopted to compare the performances of the test configurations to the reference (Default) configuration. Point estimates and corresponding 95% confidence intervals (CI) were calculated for the performance ratio of each outcome metric (propulsion cost, seat, frame, and caster vibration):

$$\rho = \frac{\text{Test Mean}}{\text{Reference Mean}} \quad (3)$$

Ratios with values of 1.00 reflect similar performance between the test and reference configurations. Ratios less than 1.00 indicate that the test configuration exhibited better performance (i.e., lower propulsion cost or vibration exposure).

To assess the meaningfulness of these ratios, the 95% CIs were compared to pre-defined upper and lower equivalence limits (UEL, LEL). The limits for propulsion cost were informed from several published studies on wheelchair propulsion efforts where human subjects were asked to propel a wide variety of wheelchair configurations including power-assisted wheels [44], lever-driven wheels [45], sports wheelchairs [46], chairs with weights added to the frame [47], [48], and with under-inflated tires [49], [50]. Across these studies, the average difference between the biomechanical outcome variables of the studies was calculated to be 9.4%. Therefore, we defined the equivalence limits as $\pm 5\%$ based on the assumption that mechanical testing is more precise than human subject investigation. Similarly, UEL and LEL values were defined for vibration exposure from published studies on wheelchair seat vibration measurements with human subjects propelling one wheelchair across different styles of sidewalk [13] and wheelchairs of different frame materials over various surfaces [32], as well daily exposure using folding or rigid MWC frames [14]. The average difference between r.m.s. vibration values for the independent variable groups was calculated to be 6.2%. Therefore, the seat, caster, and frame vibration equivalence limits were set to $\pm 6\%$.

The extents of each 95% confidence interval were compared against equivalence limits ($\pm 5\%$ for propulsion cost, $\pm 6\%$ for all vibration metrics). Confidence intervals that are completely below 0.95 (propulsion cost) or 0.94 (vibrations) were classified as 'Superior' as the test configuration experienced more preferable performance (i.e., lower propulsion costs or vibrations than the Default configuration). Conversely, confidence intervals completely above 1.05 (propulsion cost) or 1.06 (vibrations) were classified as 'Inferior'. Confidence intervals that cross one or both limits, or that reside completely within the limits, are considered 'Comparable' as the test and Default configurations exhibited similar performances. Examples of these classifications are shown in Figure 7.

TABLE II
STATISTICS AND EQUIVALENCE TEST RESULTS FOR PROPULSION COST VALUES

	Propulsion Costs (J/m)															
	Brick				Grates				Sidewalk				Tile			
	Mean	StDev	% Cha.	Class.	Mean	StDev	% Cha.	Class.	Mean	StDev	% Cha.	Class.	Mean	StDev	% Cha.	Class.
Default	13.81	1.39	-	-	20.11	2.54	-	-	14.80	0.44	-	-	13.50	0.32	-	-
FrogLeg Forks	13.50	0.64	-2.2%	Comp.	19.05	1.85	-5.3%	Comp.	13.75	0.91	-7.1%	Comp.	13.39	0.94	-0.8%	Comp.
Softroll	14.20	1.26	2.8%	Comp.	19.66	2.26	-2.2%	Comp.	15.05	0.59	1.7%	Comp.	13.95	0.48	3.3%	Comp.
MtnWheel	15.10	1.46	9.3%	Comp.	20.09	2.33	-0.1%	Comp.	14.81	0.6	0.1%	Comp.	14.12	0.54	4.6%	Comp.
SoftWheel	15.58	1.68	12.8%	Comp.	19.25	1.46	-4.3%	Comp.	16.95	1.02	14.5%	Inf.	15.78	0.97	16.9%	Inf.
LoopWheel	16.10	2.54	16.6%	Inf.	21.72	3.14	8.0%	Comp.	16.78	0.75	13.4%	Inf.	15.18	0.44	12.4%	Inf.

Bolded values represent Inferior (Inf.) or Superior (Sup.) performance compared to the Default configuration.

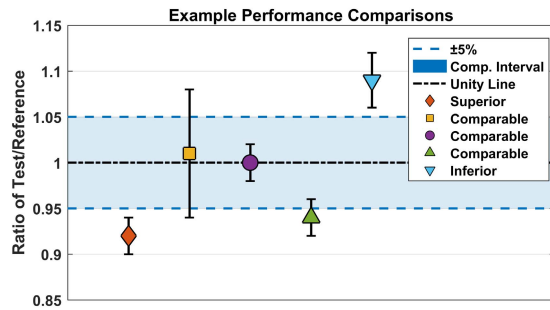


Fig. 7. Example point estimates and 95% CIs compared to $\pm 5\%$ equivalence limits, showing the three classifications.

This trichotomous analysis was conducted for all four outcome variables in Minitab (Minitab 19, Minitab LLC) with significance levels set to $\alpha = 0.05$. The Default configuration was used as the reference population. Point estimate and confidence interval values are accessible in a publicly-available database (<https://doi.org/10.35090/gatech/67086>). For ease of reader comprehension, comparisons in Tables II-V are listed as “Sup.,” “Inf.,” or “Comp.” based on these results.

IV. RESULTS

Descriptive statistics ($N = 12$ for all sets of configurations and surfaces) for propulsion cost, seat vibration, frame vibration, and caster vibration are shown in Tables II-V respectively. Shaded rows with bolded text indicate values that differ from the Default value according to the statistical analysis (i.e., classified as “Inf.” or “Sup.”).

On average, propulsion costs were comparable across tile, brick, and sidewalk (13 to 17 J/m), and higher (19 to 22 J/m) on grates. Standard deviations (StDev) were greater on brick and grates. FrogLegs Forks consistently had the lowest propulsion cost. The highest propulsion costs were between SoftWheel and LoopWheel for all surfaces. Equivalence test results identified the LoopWheel configuration to have inferior performance (i.e., higher propulsion cost values) than the Default configuration across all four surfaces. Likewise, the SoftWheel configuration had significantly higher costs over tile and sidewalk.

Table III presents descriptive statistics of the seat vibration exposure values, represented as $a_{z,(seat),r.m.s.}$. $N = 12$ for

all sets of configurations and surfaces except two trials of FrogLegs Forks over tile that were removed as outliers. The FrogLegs Forks incurred additional vibration (16-97%) at the seat across all surfaces. LoopWheel increased seat vibrations over grates by 13%. Softroll casters reduced vibration at the seat by 7-11% compared to Default over all surfaces, though grates was the only surface that showed statistically superior performance. High standard deviations and coefficients of variation on sidewalk and grates are attributed to the inconsistencies of those surfaces (i.e., random bumps).

Table IV presents the frame vibration, or $a_{z,(frame),r.m.s.}$, values, to compare across the configurations that changed the rear drive wheel of the configuration. $N = 12$ trials for each configuration. Over brick, tile, and sidewalk, the LoopWheel incurred 12-26% larger vibrations than the Default configuration. MtnWheel also increased the frame vibrations. SoftWheel was the only drive wheel to reduce frame vibrations over tile, by 11%.

The accelerometer placed at the caster stem measured the highest magnitude of vibrations. The mean $a_{z,(caster),r.m.s.}$ values are shown in Table V, averaged across $N = 12$ for the Default, FrogLegs Forks, and Softroll configurations. FrogLegs Forks increased the caster vibrations over tile by 43%. Softroll casters, conversely, significantly decreased the caster vibrations over all four surfaces by 13-27%.

Data for propulsion cost values and r.m.s. vibrations at all three measurement locations are accessible in a publicly-available database (<https://doi.org/10.35090/gatech/67086>).

V. DISCUSSION

Not unexpectedly, the five components exhibited disparate performances in the main outcome variables (propulsion cost and seat vibration) over different surfaces. The significant differences summarized in Table VI imply that many of the components specifically designed to reduce vibration exposure of MWC users were not effective at this task. In particular, SoftWheels and LoopWheels appear ineffective at vibration attenuation, even incurring 12-17% greater vibrations at the seat over most surfaces, with increased propulsion costs.

Out of the five tested components, only the Softroll casters showed any benefit to the user. Softrolls had lower seat vibration exposure than Default over Grates, without any significant increase in propulsion cost and no other apparent tradeoffs compared to Default. FrogLegs Forks increased seat vibrations on all four surfaces, without increasing propulsion cost.

TABLE III
STATISTICS AND EQUIVALENCE TEST RESULTS FOR VERTICAL VIBRATIONS MEASURED ABOVE THE MWC SEAT CUSHION

	Seat Vibrations (m/s ² , r.m.s. vertical)															
	Brick				Grates				Sidewalk				Tile			
	Mean	StDev	% Cha.	Class.	Mean	StDev	% Cha.	Class.	Mean	StDev	% Cha.	Class.	Mean	StDev	% Cha.	Class.
Default	0.53	0.02	-	-	0.55	0.04	-	-	0.50	0.03	-	-	0.30	0.01	-	-
FrogLeg Forks	0.66	0.03	24.5%	Inf.	0.68	0.03	23.6%	Inf.	0.58	0.03	16.0%	Inf.	0.59	0.06	96.7%	Inf.
Softroll	0.49	0.03	-7.5%	Comp.	0.49	0.03	-10.9%	Sup.	0.45	0.03	-10.0%	Comp.	0.28	0.01	-6.7%	Comp.
MtnWheel	0.52	0.02	-1.9%	Comp.	0.52	0.07	-5.5%	Comp.	0.47	0.04	-6.0%	Comp.	0.30	0.01	0.0%	Comp.
SoftWheel	0.52	0.02	-1.9%	Comp.	0.59	0.06	7.3%	Comp.	0.47	0.05	-6.0%	Comp.	0.30	0.01	0.0%	Comp.
LoopWheel	0.58	0.03	9.4%	Comp.	0.62	0.03	12.7%	Inf.	0.52	0.05	4.0%	Comp.	0.33	0.01	10.0%	Comp.

Bolded values represent Inferior (Inf.) or Superior (Sup.) performance compared to the Default configuration.

TABLE IV
STATISTICS AND EQUIVALENCE TEST RESULTS FOR VIBRATIONS AT THE FRAME BETWEEN DRIVE WHEEL CONFIGURATIONS

	Frame Vibrations (m/s ² , r.m.s. vertical)															
	Brick				Grates				Sidewalk				Tile			
	Mean	StDev	% Cha.	Class.	Mean	StDev	% Cha.	Class.	Mean	StDev	% Cha.	Class.	Mean	StDev	% Cha.	Class.
Default	1.09	0.05	-	-	1.27	0.11	-	-	0.79	0.13	-	-	0.27	0.02	-	-
MtnWheel	1.18	0.06	8.3%	Comp.	1.22	0.05	-3.9%	Comp.	0.87	0.05	10.1%	Comp.	0.33	0.03	22.2%	Inf.
SoftWheel	1.14	0.07	4.6%	Comp.	1.33	0.06	4.7%	Comp.	0.83	0.12	5.1%	Comp.	0.24	0.01	-11.1%	Sup.
LoopWheel	1.22	0.03	11.9%	Inf.	1.29	0.05	1.6%	Comp.	0.94	0.09	19.0%	Inf.	0.34	0.01	25.9%	Inf.

Bolded values represent Inferior (Inf.) or Superior (Sup.) performance compared to the Default configuration.

TABLE V
STATISTICS AND EQUIVALENCE TEST RESULTS FOR VIBRATIONS OVER THE CASTER STEM BETWEEN CASTER CONFIGURATIONS

	Caster Vibrations (m/s ² , r.m.s. vertical)															
	Brick				Grates				Sidewalk				Tile			
	Mean	StDev	% Cha.	Class.	Mean	StDev	% Cha.	Class.	Mean	StDev	% Cha.	Class.	Mean	StDev	% Cha.	Class.
Default	2.38	0.13	-	-	3.43	0.30	-	-	1.51	0.20	-	-	0.37	0.03	-	-
FrogLeg Forks	2.48	0.09	4.2%	Comp.	3.10	0.27	-9.6%	Comp.	1.48	0.21	-2.0%	Comp.	0.53	0.03	43.2%	Inf.
Softroll	1.96	0.09	-17.6%	Sup.	2.55	0.16	-25.7%	Sup.	1.10	0.20	-27.2%	Sup.	0.32	0.01	-13.5%	Sup.

Bolded values represent Inferior (Inf.) or Superior (Sup.) performance compared to the Default configuration.

MtnWheel showed no significant differences in performance and have higher traction than Default tires on uneven surfaces. In contrast, SoftWheels and LoopWheels both increased propulsion costs by 1.7-2.3 J/m without reducing seat vibrations over multiple surfaces. To put this into perspective, assume a user propels 1.4 km per day [17] with 90% of that motion distributed evenly across tile, brick, and sidewalk. The default configuration would incur a daily propulsion cost of 17.7 kJ, versus 20.3 kJ with the SoftWheel and 20.2 kJ with the LoopWheel. This energy is the equivalent of lifting between 167-174 different 2L bottles of water from the floor to a table-top (2.5 feet). It could be used to travel an extra 169-193 m with the Default configuration over tile, brick, or sidewalk.

In general, the seat vibrations of the Default configuration were below health guidance thresholds [51]. While FrogLegs Forks, SoftWheel, and LoopWheel had significantly higher vibrations than Default, these configurations are still well below the expected range of adverse health effects using the same style of analysis as in [51], requiring >3.5 hours of cumulative daily travel over to reach the lower extent of the health guidance caution zone [6]. Similar magnitudes of vibration exposure have been found in previous studies. For example, Chénier and Aissauoi [32] reported vertical vibrations at the seat of 0.24 m/s² over linoleum tile, and

Cooper *et al.* [18] reported seat vibration of 0.47 m/s² over poured concrete sidewalk.

Secondary outcome variables (frame and caster vibrations) also differed across components. These variables offer interesting mechanical insights to the designs of the components and of the wheelchair as a complete system. Energy-absorbing components must be engineered according to the types of accelerations that are intended to be attenuated. With respect to wheelchairs, components will have different performances according to the speed or surface. Transient impacts might be handled differently than the more steady-state vibrations experienced during WBV measurements. The commercial manufacturers of the components evaluated in this study do not fully disclose the types of surfaces, obstacles, or speeds for which the designs were optimized.

Vibration is a continuous, periodic perturbation to a system, like rolling down a tiled hallway floor, whereas shock is a sudden and infrequent impulse like impacting a door threshold. To assess shock-induced vibrations, the fourth-power vibration dose value (VDV, expressed in m/s^{1.75}) is often calculated as a complementary analysis to the basic evaluation method (r.m.s. acceleration), as described in ISO 2631-1 [6]. VDV is more sensitive to acceleration peaks than r.m.s. and is used when intermittent shock exposure is present. As a cumulative

TABLE VI
SUMMARIZED DIRECTION AND PERCENT CHANGE OF SIGNIFICANT DIFFERENCES COMPARED TO DEFAULT CONFIGURATION

	Brick		Grates		Sidewalk		Tile	
	Δ Prop. Cost	Δ Seat Vibration	Δ Prop. Cost	Δ Seat Vibration	Δ Prop. Cost	Δ Seat Vibration	Δ Prop. Cost	Δ Seat Vibration
Default	-	-	-	-	-	-	-	-
FrogLegs Forks	-	\uparrow (25%)	-	\uparrow (24%)	-	\uparrow (16%)	-	\uparrow (97%)
Softroll	-	-	-	\downarrow (-11%)	-	-	-	-
MtnWheel	-	-	-	-	-	-	-	-
SoftWheel	-	-	-	-	\uparrow (15%)	-	\uparrow (17%)	-
LoopWheel	\uparrow (17%)	-	-	\uparrow (13%)	\uparrow (13%)	-	\uparrow (12%)	-

measurement, the VDV increases with length of measurement. V DVs for this study (on average: 0.84-0.95 $\text{m/s}^{1.75}$ for brick, grates and sidewalk, 0.52 $\text{m/s}^{1.75}$ for tile) were comparable to Chénier and Aissaoui's reported V DVs for short (4 s) human propulsion trials over smooth and textured surfaces (1.14-1.60 $\text{m/s}^{1.75}$) [32] but considerably lower than measurements taken over a full 13-hour day of MWC occupancy (17.27 $\text{m/s}^{1.75}$) [14].

Literature seems to focus on fast [12], [18] and aggressive shock testing with double-drum [11], [52] and curb-drop [19], [53] experiments. To add perspective, 12.7 mm high slats on the double-drum tester impact the wheels with enough force to be used as a fatigue-to-failure test apparatus [52]. Curb-drop tests were used to evaluate shock and vibration attenuation in MWC frames with suspension systems; the results suggest that poor alignment of the suspension system to the direction of shock could worsen the vibration attenuation [19].

FrogLegs Forks, SoftWheels, and LoopWheels all feature directional spring or damper components. Perhaps proper alignment with the direction of anticipated impacts could optimize vibration attenuation and minimize the impact on propulsion cost. As they were configured in this study, however, it is possible that misalignment of the directional elements caused their poor performances.

The most evident negative effect of FrogLegs Forks was at the seat. One potential cause is that the deformation of the dampening insert within the forks may have induced a pitching moment of the MWC during the propulsion cycle and/or as the casters traversed bumps. Pitching motions would have a greater effect on higher vertical positions like the seat, especially considering the FrogLegs Forks are taller than the standard rigid forks. Propulsion-induced deformation of the fork inserts could explain why these forks imparted higher vibration than the standard rigid fork over the smooth tile surface. Double-drum testing results [11] indicate that FrogLegs Forks dissipate shocks from obstacle impacts better than rigid forks. Unfortunately, while that may be a benefit in very specific environments, our findings suggest these suspension forks worsen the continuous vibrations induced by wheelchair travel.

Literature is scarce on the vibration attenuation properties of MWC drive wheels. No differences in vibration or perceived comfort were found between MWCs equipped with Spinergy-branded spoked wheelchair wheels versus standard spoked metal wheels [38]. For wheels with built-in suspension, like LoopWheels and SoftWheels, applications outside of

MWCs had to be investigated. Bicycles use analogous wheel types to MWCs, albeit at much faster speeds of travel (e.g. 5.0-8.3 m/s versus 0.4-1.0 m/s) where vibrations and shocks are more severe [12], [18]. One bicycle simulation using SoftWheels showed significant (17-26%) reductions of vibration over asphalt and small shock-inducing obstacles, with an estimated 14% loss in efficiency at cruising speeds [54]. The cyclic compression and re-extension of the three damper spokes were identified as a periodic energy loss in rolling, as well as a cause of non-negligible pitch perturbation [54]. This periodic energy absorption likely explains the propulsion cost increases for SoftWheels and LoopWheels.

The MtnWheel was expected to reduce vibration exposure due to its wider contact patch and lower tire pressure compared to the Default pneumatic wheels. This proved to be untrue. However, MtnWheels are designed for outdoor environments (e.g., dirt and grass), where their intended benefit is the added tread and traction, rather than vibration attenuation. Overall, MtnWheels had comparable propulsion costs and seat vibrations to the Default configuration. Over smooth tile, the miniscule recurring impacts from the 'knobby' tire tread contacting the floor appeared to cause an increase in frame vibration. Vibrations transmitted from the frame to the seat must have been dampened by the cushion, as the seat vibrations were comparable between MtnWheels and Default. This suggests some vibrations from the tires are permissible without impacting the WBV exposure of the user. In future efforts, an assessment of frequency-based vibration magnitudes could be used to investigate if this damping effect from the frame, seat, and cushion shifted the acceleration frequencies present in the measured vibration. As in [19], some tradeoffs may exist where the component reduces overall shock or vibration, but shifts the vibration into frequencies most commonly associated with injury and discomfort in the human body.

Finally, the Softroll caster was expected to exhibit similar energy loss parameters as the default caster [30] with a small effect on propulsion cost [33]. Wheels lose energy primarily through hysteresis, or the cyclic deformation and restoration of infinitesimal elastomeric radial elements that make up the tire [55]. Unlike the discrete elastomeric elements of the suspension wheels and caster fork, Softroll deformation is simultaneous and omni-directional, providing a smoother ride without potential misalignment. The dampening benefit of Softrolls over the default casters is likely due to a combination of the wider contact patch and material properties, like pliability.

There are debating sources on the necessity of vibration attenuation for MWCs. No conclusive evidence exists to link MWC-induced WBVs to adverse health risks. Research on MWC travel over highly-tactile surfaces like outdoor brick walkways show high WBV values [10], [12], [13], [14], where <1 hour of travel is expected. Another study calculated WBV using the 13 hours of measured occupancy per day instead of the 1 hour of daily self-propulsion [14]. This 12-hour discrepancy greatly exaggerated the WBV value with respect to the 8-hour daily exposure thresholds. Literature suggests that wheelchair users are in motion for relatively short durations of time, about 60 minutes [15], [16], [17]. There is currently no evidence to suggest that much, if any, of this time is spent on uneven terrains that may elicit high WBV values. Furthermore, since exposure limits for wheelchair users have not been established, health risks may in fact be lower than defined by the guidelines for able-bodied workers. Rider comfort and satisfaction might also be a reason to consider energy-absorbing components, but this decision will be improved by understanding the performance under typical conditions and the impact on propulsion effort. Optimizing the MWC for propulsion efficiency is a prevailing contemporary effort in the field [30], [31], [32], [33]. Vibration attenuation could very well be a complimentary effort. The inherent tradeoffs between these parameters and the discrepancies in performance of individual components need to be considered by clinicians and users when equipping a new MWC. The question is: will the user get enough benefit from attenuating infrequent high-magnitude shocks and impacts from obstacles or curb-drops [10], [11] to justify the loss of efficiency or increase in constant vibration?

VI. LIMITATIONS

Performance of components over different surfaces, speeds, and maneuvers may change performance parameters (cost and/or vibration attenuation). The surfaces were chosen to include common surfaces (tile, and sidewalk) as well as surfaces that would impart more vibration (decorative brick and grates) and the speed of the wheelchair was reflective of the speeds measured during everyday mobility of wheelchair users [15], [16]. Surfaces with inconsistencies like a drop-off or impact with an obstacle (e.g., door threshold) are theoretically possible to test with the AMPS, but would likely have an adverse effect on the ability to measure propulsion costs. The straight trajectory used in the evaluation did not induce tire scrub, a major contributor of energy loss seen in curvilinear motion, which could impact propulsion costs.

Some components may be engineered to attenuate impacts, but the objective of the study concerned vibrations induced by over-ground movement. The test methods did not evaluate component performance during impacts, such as dropping off a curb or hitting an obstacle. Frequency analysis was not performed in this study, and could be included in future work on this topic. Furthermore, accelerometer measurements were only analyzed using the vertical (z) direction. A measure of the total magnitude of acceleration in all directions may be beneficial to account for anterior-posterior and medial-lateral vibrations. Deformation of the cushion and/or pitching moment during propulsion may have caused planar rotation of the vertical axis into the anteroposterior direction. Thus, the

linear accelerations of the system under robotic propulsion could have influenced the vertical vibrations unfairly with FrogLegs Forks. However, given the small-angle approximation, pitch angles of up to 5° are only expected to impact the measured accelerations by less than 0.4%.

VII. CONCLUSION

Manual wheelchair mobility exposes the user to whole-body vibrations that may have adverse health effects. Vibration exposure can be minimized without sacrificing the mechanical efficiency of the vehicle, though some component options have negative effects on vibrations and/or propulsion cost. In this study, robotic wheelchair propulsion permitted a repeated-measures test on wheelchair propulsion cost and vibration exposure over four common surfaces at a clinically-relevant speed. Six components with energy-absorbing characteristics were compared to standard pneumatic drive wheels and casters. Wheels with built-in suspension did not have any significant difference on vibration exposure, yet they did significantly increase the propulsion cost, effectively making the wheelchair more energetically-expensive to propel. Similarly, elastomeric suspension forks significantly increased the vibration. Out of the component options, ‘soft roll’ casters show the most promising results for ease of efficiency and effectiveness at reducing vibrations through the wheelchair frame and seat cushion. Users may define other reasons to consider energy-absorbing components, but this decision will be improved by understanding the performance under typical conditions which dominate everyday mobility.

REFERENCES

- [1] S. M. P. Verschueren, “The effects of whole-body vibration training and vitamin D supplementation on muscle strength, muscle mass, and bone density in institutionalized elderly women: A 6-month randomized, controlled trial,” *J. Bone Mineral Res.*, vol. 26, no. 1, pp. 42–49, 2011.
- [2] A. Bogaerts, C. Delecluse, S. Boonen, A. L. Claessens, K. Milisen, and S. M. P. Verschueren, “Changes in balance, functional performance and fall risk following whole body vibration training and vitamin D supplementation in institutionalized elderly women. A 6 month randomized controlled trial,” *Gait & Posture*, vol. 33, no. 3, pp. 466–472, Mar. 2011.
- [3] M. H. Pope, M. Magnusson, and D. G. Wilder, “Low back pain and whole body vibration,” *Clin. Orthopaedics Rel. Res.*, vol. 354, pp. 241–248, Sep. 1998.
- [4] O. O. Okunribido and M. M. H. Magnusson, “Pope, low back pain in drivers: The relative role of whole-body vibration, posture and manual materials handling,” *J. Sound Vib.*, vol. 298, no. 3, pp. 540–555, 2006.
- [5] T. Hansson, M. Magnusson, and H. Broman, “Back muscle fatigue and seated whole body vibrations: An experimental study in man,” *Clin. Biomech.*, vol. 6, no. 3, pp. 173–178, Aug. 1991.
- [6] *International Standards Organization, ISO 2631 Mechanical Vibration and Shock—Section 1: Evaluation of Human Exposure to Whole-Body Vibration, in Section 1: Guide for the Evaluation of Human Exposure to Whole-Body Vibration*, Standard 2631, 1997.
- [7] *Council Directive 2002/44/EC on the Minimum Health and Safety Requirements Regarding the Exposure of Workers to the Risks Arising From Physical Agents (Vibration)*, European Parliament and Council, Official Journal of the European Union (OJEU), Luxembourg City, Luxembourg, 2002.
- [8] O. Lariviere, “Vibration transmission during manual wheelchair propulsion: A systematic review,” *Vibration*, vol. 4, no. 2, pp. 444–481, 2021.
- [9] M. L. Boninger *et al.*, “Investigating neck pain in wheelchair users,” *Amer. J. Phys. Med. Rehabil.*, vol. 82, no. 3, pp. 197–202, Mar. 2003.
- [10] D. P. VanSickle, “Analysis of vibrations induced during wheelchair propulsion,” *J. Rehabil. Res. Develop.*, vol. 38, no. 4, pp. 409–421, 2001.
- [11] R. A. Cooper, E. Wolf, S. G. Fitzgerald, M. L. Boninger, R. Ulerich, and W. A. Ammer, “Seat and footrest shocks and vibrations in manual wheelchairs with and without suspension,” *Arch. Phys. Med. Rehabil.*, vol. 84, no. 1, pp. 96–102, Jan. 2003.

- [12] R. A. Cooper, "Evaluation of selected sidewalk pavement surfaces for vibration experienced by users of manual and powered wheelchairs," *J. Spinal Cord Med.*, vol. 27, no. 5, pp. 468–475, 2004.
- [13] E. Wolf, "Longitudinal assessment of vibrations during manual and power wheelchair driving over select sidewalk surfaces," *J. Rehabil. Res. Develop.*, vol. 44, no. 4, pp. 573–580, 2007.
- [14] Y. Garcia-Mendez, "Health risks of vibration exposure to wheelchair users in the community," *J. Spinal Cord Med.*, vol. 36, no. 4, pp. 365–375, 2013.
- [15] E. Wolf *et al.*, "Vibration exposure of individuals using wheelchairs over sidewalk surfaces," *Disab. Rehabil.*, vol. 27, no. 23, pp. 1443–1449, Jan. 2005.
- [16] S. E. Sonenblum and S. R. A. S. Lopez, "Manual wheelchair use: Bouts of mobility in everyday life," *Rehabil. Res. Pract.*, vol. 2012, Jul. 2012, Art. no. 753165.
- [17] S. E. Sonenblum and S. Sprigle, "Wheelchair use in ultra-lightweight wheelchair users," *Disab. Rehabil., Assistive Technol.*, vol. 12, no. 4, pp. 396–401, May 2017.
- [18] R. A. Cooper, E. Ferretti, M. Oyster, A. Kelleher, and R. Cooper, "The relationship between wheelchair mobility patterns and community participation among individuals with spinal cord injury," *Assistive Technol.*, vol. 23, no. 3, pp. 177–183, Sep. 2011.
- [19] A. M. Kwarciak, "Curb descent testing of suspension manual wheelchairs," *J. Rehabil. Res. Develop.*, vol. 45, no. 1, pp. 73–84, Dec. 2008.
- [20] S. Kitazaki and M. J. Griffin, "Resonance behaviour of the seated human body and effects of posture," *J. Biomech.*, vol. 31, no. 2, pp. 143–149, 1998.
- [21] N. Kendraoui, "Experimental investigations and finite element modelling of the vibratory compartment of a manual wheelchair," in *Proc. Int. Conf. Hum. Syst. Eng. Design, Future Trends Appl.*, vol. 876, Oct. 2018, pp. 682–688.
- [22] J. Mester, "Biological reaction to vibration—implications for sport," *J. Sci. Med. Sport*, vol. 2, no. 3, pp. 211–226, 1999.
- [23] Paralyzed Veterans of America Consortium for Spinal Cord Medicine, "Preservation of upper limb function following spinal cord injury: A clinical practice guideline for health-care professionals," *J. Spinal Cord Med.*, vol. 28, no. 5, pp. 434–470, 2005.
- [24] J. L. Mercer, "Shoulder joint kinetics and pathology in manual wheelchair users," *Clin. Biomech.*, vol. 8, no. 8, pp. 781–789, 2006.
- [25] J. D. Mozingo *et al.*, "Shoulder mechanical impingement risk associated with manual wheelchair tasks in individuals with spinal cord injury," *Clin. Biomech.*, vol. 71, pp. 221–229, Jan. 2020.
- [26] M. P. Dijkers, "Correlates of life satisfaction among persons with spinal cord injury," *Arch. Phys. Med. Rehabil.*, vol. 80, no. 8, pp. 867–876, 1999.
- [27] M. W. M. Post, L. P. de Witte, F. W. A. van Asbeck, A. J. van Dijk, and A. J. P. Schrijvers, "Predictors of health status and life satisfaction in spinal cord injury," *Arch. Phys. Med. Rehabil.*, vol. 79, no. 4, pp. 395–401, Apr. 1998.
- [28] Y. T. Wang, "Effects of wheelchair Tai Chi on physical and mental health among elderly with disability," *Res. Sports Med.*, vol. 24, no. 3, pp. 70–157, 2016.
- [29] S. E. Sonenblum, "Effects of wheelchair cushions and pressure relief maneuvers on ischial interface pressure and blood flow in people with spinal cord injury," *Arch. Phys. Med. Rehabil.*, vol. 95, no. 7, pp. 1350–1357, 2014.
- [30] S. Sprigle and M. J. H. Misch, "Measurement of rolling resistance and scrub torque of manual wheelchair drive wheels and casters," *Assistive Technol.*, vol. 34, no. 1, pp. 1–13, Dec. 2019.
- [31] J. Misch, M. Huang, and S. Sprigle, "Modeling manual wheelchair propulsion cost during straight and curvilinear trajectories," *PLoS ONE*, vol. 15, no. 6, Jun. 2020, Art. no. e0234742.
- [32] F. Chénier and R. Aissaoui, "Effect of wheelchair frame material on users' mechanical work and transmitted vibration," *Biomed. Res. Int.*, vol. 2014, Sep. 2014, Art. no. 609369.
- [33] S. Sprigle and M. Huang, "Manual wheelchair propulsion cost across different components and configurations during straight and turning maneuvers," *J. Rehabil. Assistive Technol. Eng.*, vol. 7, pp. 1–14, Apr. 2020.
- [34] *International Standards Organization, ISO 7176 Wheelchair Standards—Section 11: Test Dummies, in Section 11: Test Dummies*, Standard 7176, 2012.
- [35] J. T. Lin and S. Sprigle, "The influence of operator and wheelchair factors on wheelchair propulsion effort," *Disab. Rehabil., Assistive Technol.*, vol. 15, no. 3, pp. 328–335, 2020.
- [36] H. Liles, "Design of a robotic system to measure propulsion work of over-ground wheelchair maneuvers," *IEEE Trans. Neural Syst. Rehabil. Eng.*, vol. 23, no. 6, pp. 983–991, Nov. 2015.
- [37] S. Maeda, "Relationship between questionnaire survey results of vibration complaints of wheelchair users and vibration transmissibility of manual wheelchair," *Environ. Health Preventive Med.*, vol. 8, no. 3, pp. 9–82, 2003.
- [38] S. N. W. Vorrink, "Comparison of wheelchair wheels in terms of vibration and spasticity in people with spinal cord injury," *J. Rehabil. Res. Develop.*, vol. 45, no. 9, pp. 1269–1279, 2008.
- [39] T. G. Frank and E. W. Abel, "Measurement of the turning, rolling and obstacle resistance of wheelchair castor wheels," *J. Biomed. Eng.*, vol. 11, no. 6, pp. 462–466, 1989.
- [40] C. P. DiGiovine, R. A. Cooper, E. Wolf, S. G. Fitzgerald, and M. L. Boninger, "Analysis of whole-body vibration during manual wheelchair propulsion: A comparison of seat cushions and back supports for individuals without a disability," *Assistive Technol.*, vol. 15, no. 2, pp. 129–144, Dec. 2003.
- [41] J. Misch and S. Sprigle, "Effects of wheels and tires on high-strength lightweight wheelchair propulsion cost using a robotic wheelchair tester," *Disab. Rehabil., Assistive Technol.*, pp. 1–11, Dec. 2021, doi: 10.1080/17483107.2021.2012274.
- [42] S. Wellek, *Testing Statistical Hypotheses of Equivalence and Noninferiority*, 2nd ed. Boca Raton, FL, USA: CRC Press, 2010, p. 415.
- [43] M. P. Snow, "Comparing new designs with baselines," *Ergonom. Des., Quart. Hum. Factors Appl.*, vol. 7, no. 4, pp. 28–33, 2016.
- [44] J. Lui *et al.*, "Mechanical efficiency of two commercial lever-propulsion mechanisms for manual wheelchair locomotion," *J. Rehabil. Res. Devices*, vol. 50, no. 10, pp. 1363–1372, 2013.
- [45] E. Pavlidou, "Rolling resistance and propulsion efficiency of manual and power-assisted wheelchairs," *Med. Eng. Phys.*, vol. 37, no. 11, pp. 1105–1110, 2015.
- [46] P. A. Hilbers and T. P. White, "Effects of wheelchair design on metabolic and heart rate responses during propulsion by persons with paraplegia," *Phys. Therapy*, vol. 67, no. 9, pp. 1355–1358, 1987.
- [47] Y. Sagawa *et al.*, "Effects of wheelchair mass on the physiologic responses, perception of exertion, and performance during various simulated daily tasks," *Arch. Phys. Med. Rehabil.*, vol. 91, no. 8, pp. 1248–1254, 2010.
- [48] R. E. Cowan, "Impact of surface type, wheelchair weight, and axle position on wheelchair propulsion by novice older adults," *Arch. Phys. Med. Rehabil.*, vol. 90, no. 7, pp. 1076–1083, 2009.
- [49] S. de Groot, R. J. Vegter, and L. H. van der Woude, "Effect of wheelchair mass, tire type and tire pressure on physical strain and wheelchair propulsion technique," *Med. Eng. Phys.*, vol. 35, no. 10, pp. 1476–1482, 2013.
- [50] B. J. Sawatzky and W. O. I. K. Denison, "The ergonomics of different tyres and tyre pressure during wheelchair propulsion," *Ergonomics*, vol. 47, no. 14, pp. 1475–1483, 2004.
- [51] J. Misch and S. Sprigle, "Estimating whole-body vibration limits of manual wheelchair mobility over common surfaces," *J. Rehabil. Assistive Technol. Eng.*, vol. 9, Apr. 2022, Art. no. 20556683221092322.
- [52] *International Standards Organization, ISO 7176 Wheelchair Standards—Section 8: Requirements and Test Methods for Static, Impact and Fatigue Strengths, in Section 8: Requirements and Test Methods for Static, Impact and Fatigue Strengths*, Standard 7176, 2012.
- [53] M. Hirschke and R. F. Reiser, "Effect of rear wheel suspension on tilt-in-space wheelchair shock and vibration attenuation," *PM & R*, vol. 10, no. 10, pp. 1040–1050, Oct. 2018.
- [54] M. Corno, "Modeling and analysis of a bicycle equipped with in-wheel suspensions," *Mech. Syst. Signal Process.*, vol. 155, Jun. 2021, Art. no. 107548.
- [55] H. Pacejka, *Tire and Vehicle Dynamics*. Amsterdam, The Netherlands: Elsevier, 2005.